ICANS-XI International Collaboration on Advanced Neutron Sources
KEK, Tsukuba, October 22-26, 1990

High precision structural refinement from time-of-flight single crystal data

C C Wilson
ISIS Facility, Rutherford Appleton Laboratory, Chilton, Didcot, Oxon OX11 0QX, UK

ABSTRACT
The use of time-of-flight single crystal data in structural refinement is discussed. The advantage of variable wavelength and high $\sin\theta/\lambda$ data can lead to significantly more precise and informative refinement information. Reliable and accurate strategies for data reduction are crucial, however, and some of the complexities and possible solutions are mentioned.

I. INTRODUCTION

Pulsed source single crystal diffraction has, by its nature, several features which are of benefit in structural refinement:

(i) The collection of many Bragg reflections simultaneously in the detector allows the accurate determination of crystal cell and orientation from a single data histogram (collected in one fixed crystal/detector geometry). It should also be noted that for some applications this single histogram may be the only data required;

(ii) The white nature of the incident beam enables the straightforward measurement of reflections at different wavelengths. This ability is invaluable in the precise study of wavelength dependent effects such as extinction and absorption;

(iii) The collection of data to the very high $\sin\theta/\lambda$ values accessible on SXD (exploiting the high flux of useful epithermal neutrons from the undermoderated ISIS beams) allows more precise parameters to be obtained, enabling the examination of very subtle structural features.

For many problems in physics, the refinement parameters required are not the normal positional and vibrational parameters, but may be (or may be classed as) second, or higher, order effects. For example, disordered structures, higher order potential terms, incommensurate or satellite peaks, new minority phases etc. In order to be able to extract parameters such as these reliably and precisely, it is necessary both to extract accurate diffraction intensities to very high Q and to apply all necessary corrections to these data in the reduction to a set of structure factors for refinement.

II. DATA EXTRACTION AND REDUCTION

The extraction of structure factor information from an SXD data set proceeds in two stages. Given the provision of an accurate UB matrix from the earlier stages of the data processing procedure, integrated intensities are extracted from the raw data using Wilkinson's modification of the $\sigma(I)/I$ method (Wilkinson, 1986; Wilkinson et al, 1988). This procedure involves fitting variable-shaped ellipsoidal integration volumes around the reflection position as predicted from the crystal UB matrix. Local interpolation of the peak centroid improves the integration accuracy and can also be used to improve the quality of the UB matrix. The "learning" of the shapes of the stronger reflections is exploited by imposing these shapes upon the profiles of weaker reflections occurring in similar regions on the detector. The use of this peak shape library method allows significantly more reliable weak intensities to be extracted, along with the benefit of more accurate strong intensities from the application of the $\sigma(I)/I$ technique. Since

reflections at high Q tend to be rather weak, the availability of data at very high $\sin\theta/\lambda$ values of $>2\text{Å}^{-1}$ on SXD depends strongly on the successful and reliable extraction of weak peak intensities.

Once a reliable set of integrated intensities has been extracted from the raw data, it is necessary to reduce these to structure factors. For this we use the formula of Buras and Gerward (1975)

$$I_h = i_o(\lambda)\, V\, N^2\, |F_h|^2\, \lambda_h^4\, \epsilon(\lambda,\alpha)\, A_h(\lambda)\, E_h(\lambda) / 2\sin^2\theta_h \qquad (1)$$

where

I_h is the measured intensity of reflection h;
$i_o(\lambda)$ is the incident flux;
V is the crystal volume;
N is the number density of unit cells;
$|F_h|$ is the structure factor magnitude of reflection h;
λ_h is the wavelength at which h is measured (λ^4 is reflectivity);
$\epsilon(\lambda,\alpha)$ is the detector efficiency, a function of wavelength and detector coordinate $[\alpha = \alpha(x,z)]$;
θ_h is the Bragg angle at which h is measured (The term $1/2\sin^2\theta_h$ is the Lorentz correction. It should be noted that in time-of-flight Laue diffraction, the "moving" part to which this correction refers is the contraction of the Ewald sphere (radius $1/\lambda$) during the pulse time frame);
$A_h(\lambda)$ is the absorption correction;
$E_h(\lambda)$ is the extinction correction.

In practice on SXD at present this data reduction is accomplished in three stages :

(i) The detector spatial response correction $\epsilon[\alpha(x,z)]$ is taken account of within the peak integration program;

(ii) In the main reduction program SXDRED, the expression evaluated is

$$|F_h| = \{I_h\, 2\sin^2\theta_h / (i_o(\lambda)\, V\, N^2\, \lambda_h^4\, \epsilon(\lambda)) \qquad (2)$$

(iii) In the Cambridge Crystallographic Subroutine Library (CCSL; Brown and Matthewman, 1987) routine TOFEA, the coefficients for the evaluation and subsequent refinement of wavelength and path length dependent absorption and extinction corrections are calculated.

Structure factor refinement is then carried out within the framework of CCSL using the least squares program SFLSQ. In addition, of course, the flexibility of the CCSL system allows special features to be conveniently built in to a refinement, such as bond constraints, relations between variables, magnetic structures etc.

III. FURTHER DATA CORRECTION - THERMAL DIFFUSE SCATTERING

Thermal diffuse scattering (TDS) can be examined in detail using SXD. For a time-of-flight experiment the TDS around an elastic peak displays an appearance characterised by the ratio of the velocity of sound in the crystal to the neutron velocity. Early work on this phenomenon was carried out on HRPD at ISIS in backscattering geometry (Willis et al, 1986) but there are considerable changes in the phonon spectrum as the scattering geometry changes on SXD. Measurements of this effect (Figure 1) are made possible on SXD as a result of the extremely low background close to the Bragg peaks obtained using the ZnS fibre-optic encoded PSDs.

It is hoped that a detailed understanding of such TDS processes and their wavelength and geometry dependence will enable more accurate corrections to be made to intensities collected on SXD. The use of both empirical and analytical models for the TDS under Bragg peaks is being investigated.

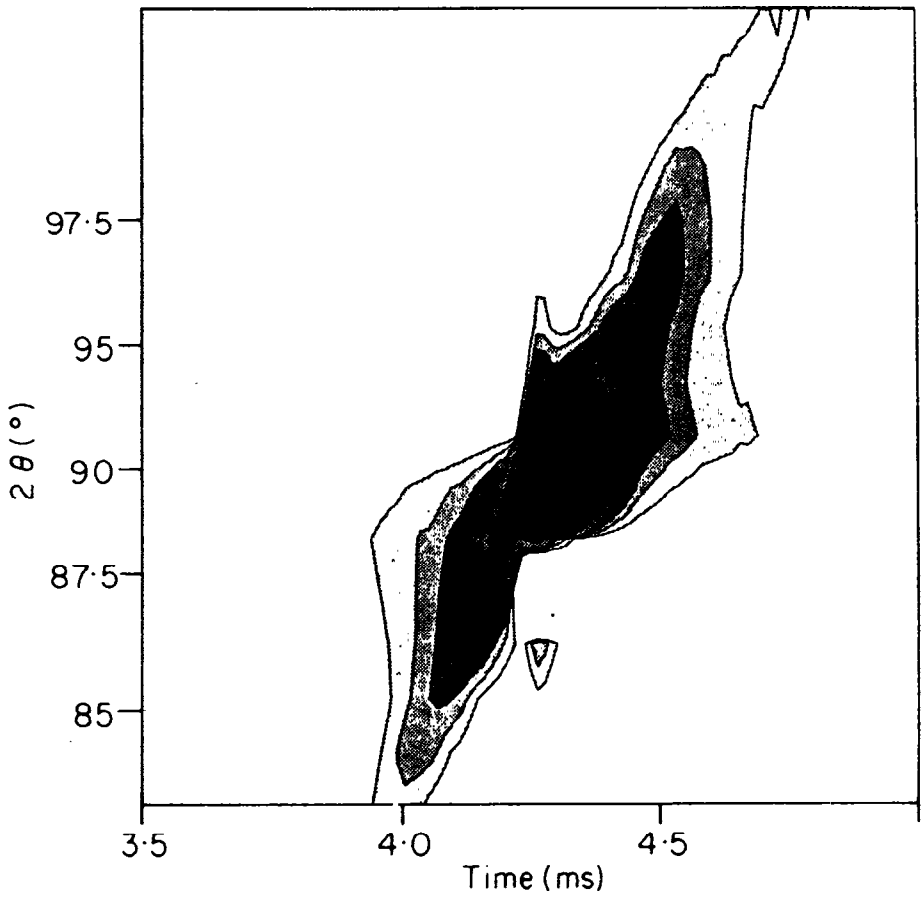

Figure 1 – The thermal diffuse scattering around the (004) reflection of SrF_2 as measured on SXD. Note the presence of the one phonon branch and the obvious anisotropy of the correction required for this effect.

IV. PROFILE EXTRACTION OF INTENSITIES

The question of subtraction of TDS corrections of the type shown in Figure 1 illustrates the desirability of utilising the 3D peak shape information inherently available in time-of-flight single crystal diffraction. Clearly to correct satisfactorily for scattering processes of this type one should do more than simply integrate over some averaged integration volume shape. Ideally one would correct point-by-point in Q-space. Once this is contemplated, the obvious next step is to extract integrated intensities by a full 3D profile fitting procedure, analagous to the Pawley method in powder diffraction (Pawley, 1981), in which detailed peak shape knowledge is used to optimise intensity extraction.

The potential for this method of intensity extraction has been illustrated using the (00l) row of the W-type hexaferrite $Ba(Fe,Co)_2Fe_{16}O_{27}$ (c-axis length = 32.9Å). In this case, accurate intensities were extracted as far as the (0,0,80) reflection, into a region where the diffraction peaks from this material measured on SXD are very significantly overlapped. The high $\sin\theta/\lambda$ values made accessible by this technique should substantially improve the potential resolution of SXD data sets, in addition to allowing detailed Q-dependent corrections to be made. Work on the 2D and 3D profile methods is in progress, especially in relation to intensity extraction from the large unit cell materials intended for study on the proposed biological diffractometer DIBS.

V. STRUCTURAL STUDY OF SrF_2 – EXTINCTION AND ANHARMONICITY

For this experiment (Forsyth, Wilson and Sabine, 1989) a cylindrical sample (height 8mm, diameter 2.5mm) of the fluorite material SrF_2 mounted along $<1\bar{1}0>$ was used. In this case

data were collected solely in the equatorial plane of the instrument, allowing access to (hhl) reflections. The scattering angles for the data collection ranged from 50–110° in 2θ, and the wavelength range from 0.36–6Å. The resulting 101 reflections were used in SFLSQ to refine the structural parameters (Wilson and Forsyth, 1989). It should be noted that not all of these reflections have unique h,k,l values. Since identical reflections measured at different wavelengths remain distinct observations until all wavelength dependent terms are corrected for and since in this case extinction is refined in the least squares program, these reflections are used separately in the refinement data set. Extinction was corrected for using a variable wavelength adaptation of the CCSL extinction correction routine using a Becker–Coppens Gaussian model, with one variable parameter. The refined parameters are shown in Table 1.

TABLE 1 – Refined SrF_2 structural parameters

Scale	9.13
B_{Sr}	0.470(26) Å^2
B_F	0.732(31) Å^2
mosaic spread	1.03(10) 10^{-4} rad^{-1}
R (unweighted)	0.050

On completion of this refinement, however, it was clear that allowance for anharmonic thermal vibrations of the fluorine atoms would significantly improve the quality of the fit. In this model, the thermal vibrations of the tetrahedrally bound fluorine atoms in the SrF_2 structure are defined by the potential

$$V_F(\underline{r}) = V_{0F} + \tfrac{1}{2}\alpha_F(x_F^2 + y_F^2 + z_F^2) + \beta_F(x_F y_F z_F) \qquad (3)$$

where x_F, y_F, z_F are the displacement coordinates for the thermal vibrations of the fluorine atom. It can be shown (Mair and Barnea, 1971) that the third order term β_F has a significant effect on the intensities of reflections where the sum of indices $|h|+|k|+|l| = 4n\pm1$. The ratio of two structure factors of this type can be written as

$$F_+/F_- = 1 - (2b_F/b_{Sr}) \exp\{(B_{Sr}-B_F)[(h^2+k^2+l^2/4a^2)]\} \times (B_F/4\pi a)^3 (\beta_F/kT)[|h_1k_1l_1| + |h_2k_2l_2|] \qquad (4)$$

where

$|F\pm|$ are the structure factors for reflections with $|h|+|k|+|l| = 4n\pm1$;
b_{Sr}, b_F are the scattering lengths of Sr and F;
B_{Sr}, B_F are the isotropic temperature factors;
a is the cubic cell parameter;
k is the Boltzmann constant;
T is the absolute temperature;
β_F is the anharmonicity parameter for fluorine.

It can be seen from this that if one measures pairs of reflections with equal $(h^2+k^2+l^2)$, which in the harmonic approximation have equal intensities, then by (4) some intensity variation can be expected for pairs whose $|h|+|k|+|l| = 4n\pm1$ (see Figure 2). It can also be seen from equation (4) that the effect becomes more pronounced at higher Q – this is where the ability of SXD to exploit the useful ISIS epithermal flux and access the highest resolution data becomes especially valuable. The very high $\sin\theta/\lambda$ attainable on SXD should allow greater precision to be obtained in the determination of the anharmonicity parameter β_F.

To examine this effect, further data were collected on SXD consisting of: 69 (hhl) reflections measured in a full 360° ω scan, with all 4 symmetry equivalent reflections averaged; and 19 further reflections of the $4n\pm1$ type discussed above, which are expected to exhibit the effects of anharmonicity in a pronounced way and were collected at higher statistics. The latter set of reflections do indeed demonstrate significant anharmonic effects, as illustrated in Table 2.

Figure 2 – The $(3,3,\bar{15})$ (top) and $(9\bar{9}9)$ reflections of SrF_2. In the harmonic approximation these two reflections would have equal intensities. The observed intensity difference is due to the anharmonic thermal vibrations exhibited by the fluorine atoms.

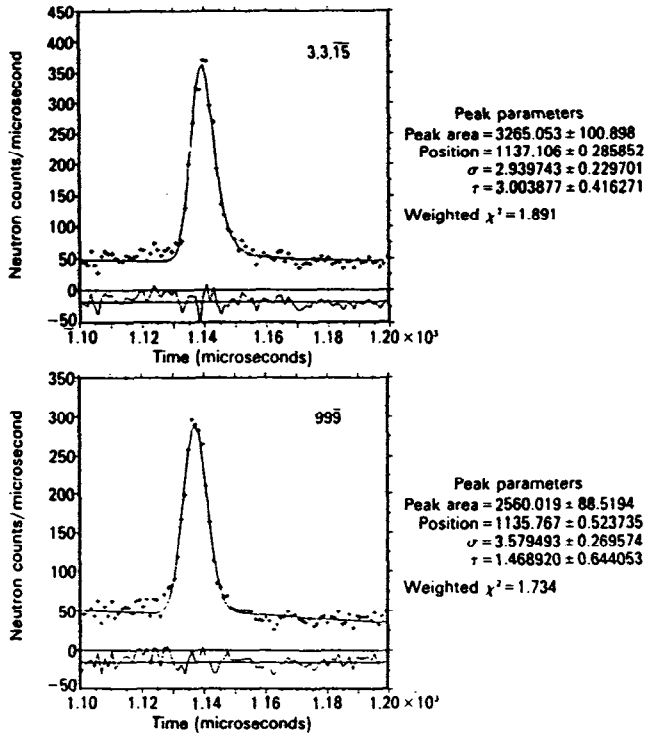

TABLE 2 – Anharmonicity affected pairs of reflections measured for SrF_2

The 'expected' values in this table were calculated using the Cooper and Rouse value of β_F, the 'calculated' values using the refined value from the SXD data.

$\Sigma(h^2+k^2+l^2)$	Pair		RATIO (F_+/F_-) Expected	Measured	Calculated
99	(5 5 7)	(4n+1)	1.045	1.042(4)	1.047
	(3 3 9)	(4n-1)			
	(5 5 7)	(4n+1)	1.039	1.043(5)	1.041
	(7 7 1)	(4n-1)			
123	(1 1 11)	(4n+1)	1.042	0.996(5)	1.045
	(7 7 5)	(4n-1)			
171	(5 5 11)	(4n+1)	1.043	1.032(6)	1.046
	(1 1 13)	(4n-1)			
187	(3 3 13)	(4n-1)	1.000	0.983(8)	1.000
	(9 9 5)	(4n-1)			
219	(7 7 11)	(4n+1)	1.119	1.160(19)	1.126
	(5 5 13)	(4n-1)			
243	(3 3 15)	(4n+1)	1.113	1.107(11)	1.120
	(9 9 9)	(4n-1)			
	(3 3 15)	(4n+1)	1.034	1.044(9)	1.036
	(11 11 1)	(4n-1)			
323	(7 7 15)	(4n+1)	1.205	1.308(31)	1.217
	(11 11 9)	(4n-1)			
363	(11 11 11)	(4n+1)	1.226	1.207(45)	1.240
	(13 13 5)	(4n-1)			
	(1 1 19)	(4n+1)	1.090	1.110(40)	1.095
	(13 13 5)	(4n-1)			

Maximum $\sin\theta/\lambda = 1.696$ Å^{-1} ($Q = 21.2$ Å^{-1})

The anharmonicity refinements were carried out in an adaptation (Mair and Barnea, 1971) of the ORFLS program (Busing, Martin and Levy, 1962), using data pre-corrected for extinction in CCSL. The results of the refinements are summarised in Table 3.

TABLE 3 - Anharmonicity refinements on SrF_2

Reflections used	Anharm Refined	Scale Factor	B_{Sr} (Å2)	B_F (Å2)	β_F (x10^{-19} J.Å^{-3})	R
ALL (88)	NO	1.006(8)	0.454(11)	0.737(16)		0.0425
ALL (88)	YES	1.007(6)	0.457(10)	0.737	-5.0(1.5)	0.0388
4n±1 (16)	NO	1.100(41)	0.539(30)	0.732		0.0441
4n±1 (16)	YES	1.107(9)	0.539	0.732	-4.02(28)	0.0219

The improvements in fit are apparent in both cases, but are of course especially emphasised when only those pairs of reflections exhibiting anharmonicity are used.

The β_F parameter obtained from the refinement should be compared with that obtained from a least squares fit of the observed F_+/F_- ratios (-4.19(30) 10^{-19} J.Å^{-3}) and the previous determination by Cooper and Rouse (1971) (-3.95(46) 10^{-19} J.Å^{-3}) from reactor data. These determinations of the β_F parameter agree well with each other, but it is plain that the *precision* of the SXD determination is higher, reflecting the high $\sin\theta/\lambda$ reached (1.7Å^{-1}) compared with that attained in the earlier study (0.9Å^{-1}).

VI. REFINEMENT OF RELAXED FLUORINE ION POSITIONS IN $(Ca,Y)F_{2.05}$

The doping of 5% YF_3 into CaF_2 introduces interstitial fluorine ions into the lattice. These interstitials cause relaxation of neighbouring fluorine atoms residing on normal tetrahedral fluorite anion sites. The principal interest in the study of these potential fast-ion conduction materials is in the examination of the coherent diffuse scattering caused by the formation of these defect clusters. However, since the relaxation of these ions is, on average, coherent throughout the sample, the diffraction, or structure factor, data also contains information on the geometry of the relaxed ions. It is obvious that the two types of information do not exist in isolation but that the same model ought to be derived from both diffuse and diffraction data.

To this end, in a recent experiment on SXD, two sets of data were collected from the CaF_2-5%YF_3 system, from two crystals grown from the same solid solution. Data from the larger of the two crystals was used in studying the diffuse scattering and diffraction data were accumulated from a smaller, cylindrical crystal (height 10mm, diameter 3mm). Both data sets were collected close to the equatorial plane of SXD from samples mounted along $<1\bar{1}0>$, allowing access to reflections close to the (hhl) plane. A total of 116 $|F_h|$ values were used in these preliminary structural refinements, to a maximum $\sin\theta/\lambda$ of 1.45 Å^{-1}.

The initial model used was based on that of Cheetham et al (1971), with the interstitial fluorine atom F' displaced along the $<110>$ direction and the relaxed F'' ion alone $<111>$ (Figure 3). The diffraction data will of course merely give a crystal average for these relaxations - it is the aim of the diffuse scattering to reveal the local clustering arrangement.

These initial refinements were successful, with values obtained for fluorine positions, thermal parameters and site occupancies which were in good agreement with the previous work (see Table 4). At this stage, however, a more extended model of the cluster was obtained from the diffuse scattering data which introduced further relaxed fluorine ions in two next neighbour positions. From the diffuse scattering data these ions, F''_b and F''_c, both again relaxed along $<111>$, had coordinates of (0.28,0.28,0.28) and (0.26,0.26,0.26). Such is the nature of the

relaxed ion "tree" introduced by the initial interstitial F' ion, that there are 2 F" ions, 6 F"$_b$ ions and 16 F"$_c$ ions in this model. The residual F atom occupancy on the original tetrahedral site is now as low as 0.46.

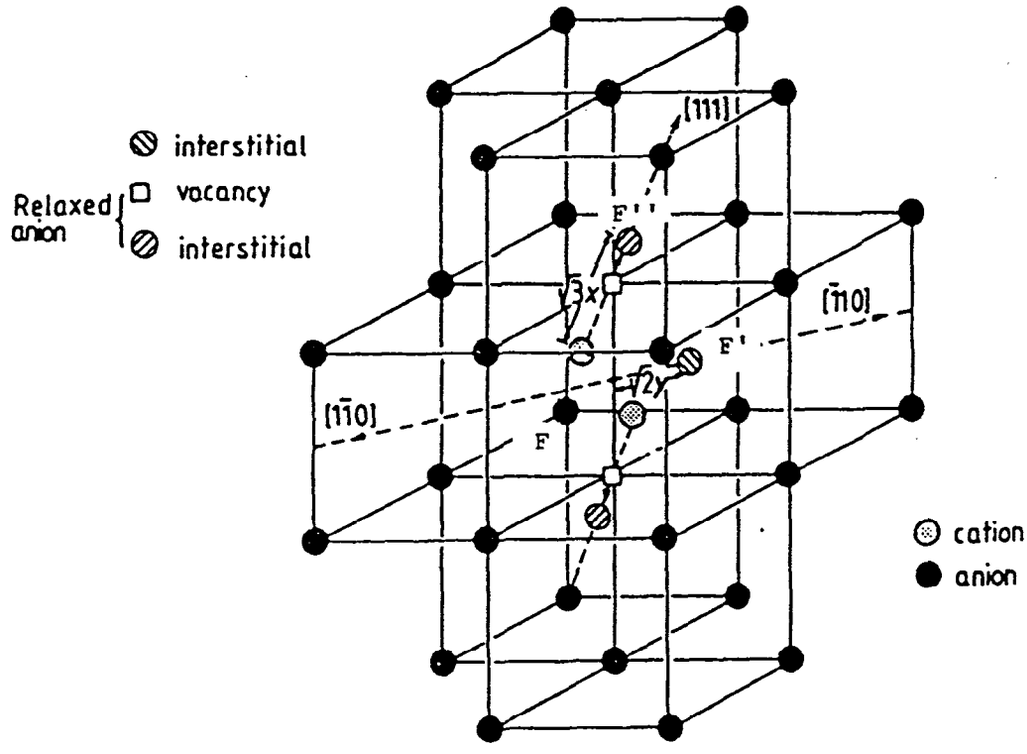

Figure 3 – A model for the defect cluster in (Ca,Y)$F_{2.05}$, showing the interstitial F' ion positions and the relaxed interstitials F".

TABLE 4 – Preliminary refinement results for CaF_2–5%YF_3
116 observations, 9 variables, R = 6.83%
Scale = 62.5(22), Mosaic Spread = 0.56(9) 10^{-4} rad^{-1}

Atom	x/a	y/b	z/c	B_{iso} (Å^2)	Site	F_{2+x}
Ca	0.0	0.0	0.0	0.684(41)		
F	0.25	0.25	0.25	0.881(37)	0.970(18)	1.94(4)
F'	0.5	0.377(4)	0.377(4)	0.65(6)	0.0058(14)	0.070(15)
F"	0.407(16)	0.407(16)	0.407(16)	0.65*	0.0057(14)	0.046(12)

The introduction of this model leads to the refined parameters given in Table 5, and a slightly reduced R-factor of some 6.5%. The data reduction in this case was carried out rapidly on this recently collected data and with care the intensity information should improve. The most impressive aspect of the preliminary refinement, by now involving a highly distorted structure, is the stability of the F"$_b$ and F"$_c$ positional coordinates, which are refined straightforwardly from the data in spite of their small deviations from the tetrahedral site and their rather low occupancies. The refined coordinates for these 2nd and 3rd neighbour relaxed ions agree fairly well with the values obtained from the diffuse scattering data fit. This gives some confidence that the interstitial–relaxed ion model being proposed is fairly close to the true defect cluster.

TABLE 5 - Preliminary refinement results for CaF_2–5%YF_3
Using extended interstitial 'tree', R = 6.52%
Scale = 64.3(11), Mosaic Spread = 0.75(9) 10^{-4} rad^{-1}

Atom	x/a	y/b	z/c	B_{iso} ($Å^2$)	Site	F_{2+x}
Ca	0.0	0.0	0.0	0.682(34)		
F	0.25	0.25	0.25	0.828(43)	0.464	0.93
F'	0.5	0.370(9)	0.370(9)	0.60(6)	0.0058	0.070
F"	0.403(11)	0.403(11)	0.403(11)	0.60*	0.0057	0.048
$F"_b$	0.266(3)	0.266(3)	0.266(3)	0.60*	0.0340	0.272
$F"_c$	0.258(5)	0.258(5)	0.258(5)	0.60*	0.0910	0.728

The use of high Q single crystal diffraction data in this way to obtain fairly precise positional parameters for slightly disordered ions is a good example of structural refinement on SXD. Coupled with the simultaneous measurement of the coherent diffuse scattering pattern, it shows the great power and versatility of the instrument in such studies of total elastic scattering.

References

Brown P J and Matthewman J C, Rutherford Appleton Laboratory Report, RAL-87-010 (1987)
Busing W R and Levy H A, Acta Cryst. 22, 457 (1967)
Cheetham A K, Fender B E F and Cooper M J, J. Phys. C 4, 3107 (1971)
Cooper M J and Rouse K D, Acta Cryst. A27, 622 (1971)
Forsyth J B, Wilson C C, Stringer A M, Howard J A K and Johnson O, J. de Phys. Colloque C5-47, 143 (1986)
Forsyth J B, Wilson C C and Sabine T M, Acta Cryst. A45, 244 (1989)
Pawley G S, J. Appl. Cryst. 14, 357 (1981)
Wilkinson C, J. de Phys. Colloque C5-47, 35 (1986)
Wilkinson C, Khamis H W, Stansfield R F D and McIntyre G J, J. Appl. Cryst. 21, 471 (1988)
Willis B T M, Carlile C J, Ward R C, David W I F and Johnson M W, Europhys. Letts. 2, 767 (1986)
Wilson C C and Forsyth J B, Rutherford Appleton Laboratory Report RAL-89-005 (1989)